



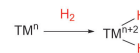
Polar X–H Bond (X=O, S, N) Activation at a Cage Silanide

Pamela Adienes Benzan Lantigua, Martin Lutz, and Marc-Etienne Moret*

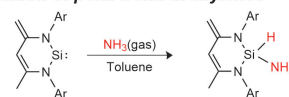
Abstract: Low-valent silicon compounds such as neutral silylenes display versatile reactivity for the activation of small molecules. In contrast, their anionic congeners silanides ($[\text{R}_3\text{Si}^-]$) have primarily been investigated for their nucleophilic reactivity. Here we show that incorporating a silanide center in a bicyclic cage structure allows for formal oxidative addition of polar element-hydrogen bonds (RX-H , R =aromatic residue, $\text{X}=\text{O}, \text{S}, \text{NH}$). The resulting hydrosilicates were isolated and characterized structurally and spectroscopically. Density Functional Theory (DFT) calculations and experimental observations support an ionic mechanism for RX-H bond activation. Finally, the reactivity of the RS-H bond adduct was further investigated, revealing that it behaves as a Lewis pair upon facile heterolytic cleavage of the Si-S bond.

Metal-free catalysts based on main group elements are attracting attention as potential contributors to more environment-friendly synthetic routes for chemicals. Of particular interest are main group species possessing geometrically close donor and acceptor orbitals separated by low energy gaps, which crudely mimic the frontier orbitals of transition metal (TM) compounds (Figure 1a).^[1,2] A seminal example is constituted by Frustrated Lewis Pairs (FLPs), which combine electron-deficient (Lewis acidic) and electron-rich (Lewis basic) centers that do not form adducts because of sterically demanding substituents. The Lewis amphoteric character of FLPs allows them to capture and/or activate various small molecules.^[3] Compounds in which this Lewis amphoteric character is concentrated on a single atom are especially attractive as TM mimics. For example, certain singlet carbenes are able to activate a H_2 molecule that interacts with both a vacant orbital and an electron lone pair

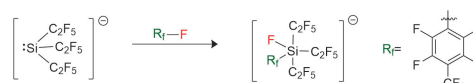
a) Oxidative addition at a transition metal complex



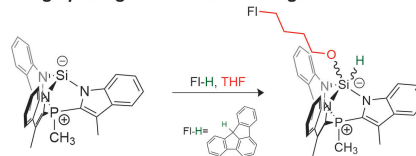
Oxidative addition of polar bond at silylenes



c) C–F oxidative addition at a silanide



d) THF ring opening at a zwitterionic cage silanide



e) This work: element-hydrogen oxidative addition at a cage silanide



Figure 1. Example of reported oxidative addition with different systems (a, b, c), example of THF ring opening at a zwitterionic silanide (d), and this work (e).

in a geometrically perpendicular orbital.^[4] Heavier analogues, such as neutral Si(II) compounds (silylenes), are emerging as versatile reagents for the activation of small molecules. Recent examples include the activation of small molecules (H_2 , CO_2 , N_2O), of polar bonds as N-H in NH_3 (Figure 1b) or hydrazine or O-H in water or alcohols, as well as various other functional groups such as ketones, aldehydes, alkenes, and alkynes.^[2,5–25]

In comparison with their neutral congeners, anionic Si(II) compounds (silanides, $[\text{R}_3\text{Si}^-]$) have been less investigated for bond activation. As a rule, they primarily display nucleophilic reactivity, which makes them useful synthetic intermediates in organosilicon chemistry.^[26,27] Krempner has recently shown that zwitterionic silanides can form adducts with Lewis acids,^[28] and Cowley has demonstrated a promising catalytic application of the $(\text{Me}_3\text{Si})_3\text{Si}^-$ anion to the hydroboration of C=O bonds.^[29] One demonstrated way to affect the electronic properties of a Si center is the

[*] P. A. Benzan Lantigua, Dr. M.-E. Moret
 Organic Chemistry and Catalysis, Institute for Sustainable and
 Circular Chemistry,
 Faculty of Science, Utrecht University
 Universiteitsweg 99, 3584 CG, Utrecht (The Netherlands)
 E-mail: m.moret@uu.nl

Dr. M. Lutz
 Structural Biochemistry, Bijvoet Centre for Biomolecular Research
 Faculty of Science, Utrecht University
 Universiteitsweg 99, 3584 CG, Utrecht (The Netherlands)

© 2024 The Authors. *Angewandte Chemie International Edition*
 published by Wiley-VCH GmbH. This is an open access article under
 the terms of the Creative Commons Attribution License, which
 permits use, distribution and reproduction in any medium, provided
 the original work is properly cited.

incorporation of strongly electron-withdrawing perfluorinated substituents.^[30,31] Two recent studies by the group of Hoge showed that silanides bearing strongly electron withdrawing perfluoroalkyl groups display reactivity consistent with a Lewis-amphoteric character.^[33,34] In particular, they undergo oxidative addition of C–F bonds (Figure 1c) and addition to C=O bonds to form silaepoxides.

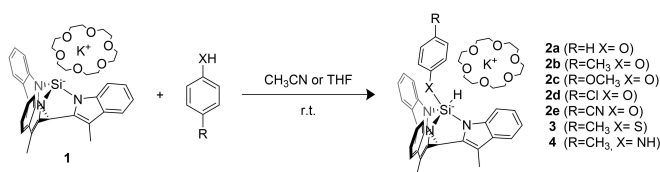
Our group has recently shown that incorporation of a silanide in a strained cage structure stabilizes the anionic center and renders unusual reactivity possible. In particular, the zwitterionic cage silanide tsmP₃Si (tsmpH₃=tris(2-skatyl)methylphosphonium) reacts with C–H acids in THF to form ring opening products via nucleophilic attack on a THF molecule coordinated to the protonated silanide [tsmpSiH]⁺ (Figure 1d).^[35] In this process, the Si center sequentially acts as a nucleophile (base) and then as an electrophile (Lewis acid) to activate relatively unreactive molecules.^[35] These results demonstrate the ability of such cage structures to support both the Si^{II} and Si^{IV} oxidation states, and hint at their potential for bond activation and catalysis.

Here we report on the reactivity of a cage silanide derived from tris-(3-methylindol-2-yl)methane (tmimH₃) with polar element-hydrogen bonds (X–H, X=O, S, NH), leading to pentacoordinate hydrosilicates by oxidative addition (Figure 1e). The mechanism of X–H bond activation is discussed based on Density Functional Theory (DFT) calculations, supporting a primarily ionic process. We also

describe the fluxional behavior and further reactivity of the products.

Treatment of silanide **1**^[27] with an equimolar amount of X–H substrate (phenol, *p*-cresol, *p*-methylthiophenol, *p*-toluidine) at room temperature led to the clean isolation of oxidative addition products [K(18-crown-6)] [(tmim)SiH(XC₆H₄R)] **2a**, **b**, **3**, and **4** in which the formal oxidation state of the Si center changed from II to IV (Scheme 1). To investigate electronic effects, the reaction of compound **1** with different *p*-substituted phenols was followed via NMR at room temperature. In each case, rapid formation of the corresponding hydrosilicate was observed, highlighting that the reaction tolerates a range of different substituents (See Supporting Information section 3.2). Of note, exposing **2a** to an excess of *p*-cresol leads to full protonolysis of the Si–N bonds with concomitant release of H₂. The product of the reaction was identified as complex salt [(18-crown-6)K]⁺ [(PhO)(tmimH₃)][−] by X-ray crystallography (See Supporting Information Section 3.1). The observed H₂ is most likely formed by protonation of the Si–H bond in **2a**, illustrating its hydridic character.

The isolated oxidative addition products were characterized by multinuclear NMR spectroscopy, FTIR, and X-ray crystal structure determination for **2a**, **3**, and **4**. The geometry of all the compounds (Figure 2) can be described as a slightly distorted trigonal bipyramid (TBP) with 2 N atoms from the tmim fragment and the H atom in the equatorial position. The remaining N and the X fragment are in the axial position, with an almost linear N–Si–X angle (X=O, 171.80°; X=S, 174.66°, X=NH, 172.80°). While the phenolate and thiophenolate moieties in **2a** and **3** are the most electronegative and therefore the most apicophilic substituents, the axial position of the anilide substituent in **4** is likely imposed by the fact that the tmim ligand cannot occupy both axial positions. IR spectra of the hydrosilicates display broad signals at 2224 cm^{−1} (**2a**), 2238 cm^{−1} (**3**) and 2066 cm^{−1} (**4**) that correspond to the Si–H vibrations (See Supporting Information section 3.8).



Scheme 1. Reaction of silanide **1** with 1 equiv. of substrate.

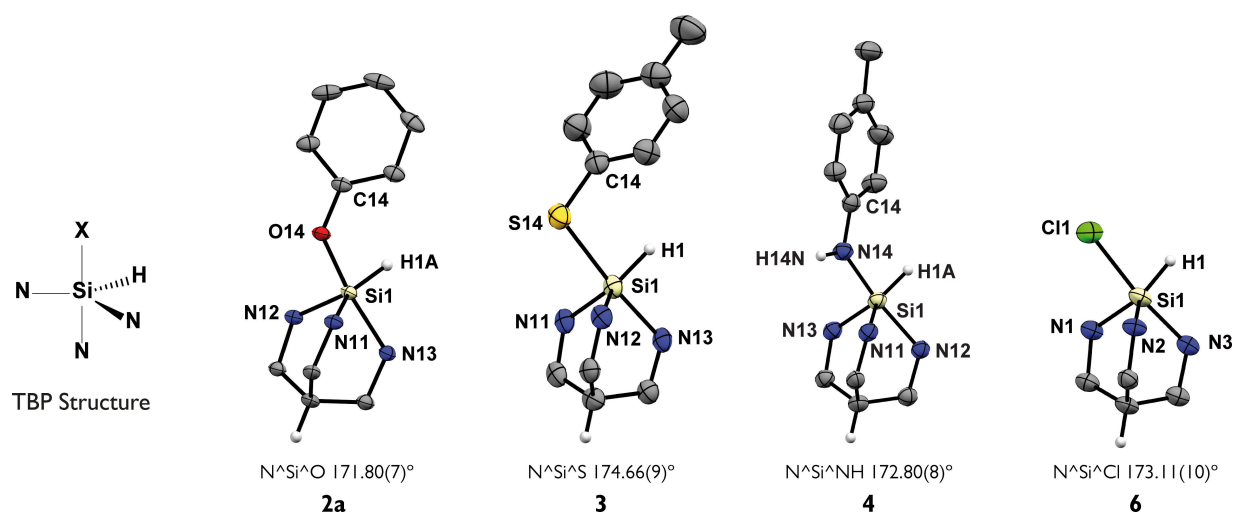


Figure 2. Molecular structures of compound **2a**, **3**, **4** and **6**. Displacement ellipsoids are drawn at the 50% probability level. Counteranion, solvents and not relevant hydrogen atoms were omitted for clarity.^[39] Only the core structure is represented for all the compounds.

Solution NMR data for **2a** support a similar structure as in the solid-state. Namely, ^1H NMR spectra in MeCN-d_3 display signals corresponding to the tris-(3-methylindol-2-yl)methane (tmim) fragment, one phenolate moiety, and an additional signal at 7.17 ppm that is not bonded to a C atom and corresponds to the newly formed Si–H bond (see Supporting Information, Section 6). The ^{29}Si NMR spectrum shows a signal at -121.0 ppm, consistent with a pentacoordinated Si center.^[32,35] A large $^1J(^{29}\text{Si}-^1\text{H})$ coupling (311 Hz) measured by ^{29}Si -INEPT (Insensitive Nuclei Enhanced by Polarization Transfer) for **2a** confirms the presence of a Si–H bond and indicates a high s character in the Si–H bonding orbital, consistent with the hydrogen atom occupying an equatorial position in a pentacoordinate trigonal bipyramidal (TBP) structure.^[36] The NMR parameters related to the Si–H unit respond distinctly to substituent effects on the phenolate moiety (See Supporting Information Table S1): from the most electron-withdrawing ($-\text{CN}$) to the most donating ($-\text{OMe}$) substituent, δ (^{29}Si) increases from -122.9 to -120.4 ppm, δ (^1H) decreases from 7.25 to 7.12 ppm, and $^1J(^{29}\text{Si}-^1\text{H})$ decreases from 324 to 307 Hz.

Interestingly, all three 3-methylindolide arms of the tmim ligand in **2a–e** appear equivalent in ^1H and ^{13}C NMR spectra, in apparent contradiction with the TBP structure observed in the solid state. This observation suggests that exchange of the apical and equatorial N atoms by Berry-like pseudorotation^[37] is rapid on the NMR time scale, as was previously observed with related compounds bearing the tsmip ligand.^[35]

Solution NMR data for **3** is indicative of an additional chemical exchange process. A ^1H NMR spectrum in THF-d_8 shows a series of sharp signals belonging to the tmim fragment, and some broad signals corresponding to the thiolate moiety. The Si–H moiety is characterized by a ^1H NMR signal at 8.20 ppm, a broad ^{29}Si signal at -102.8 ppm, and a $^1J(^{29}\text{Si}-^1\text{H})$ of 385 Hz, indicating that the hydrogen atom occupies an equatorial position. Cooling the sample down to -80°C results in sharpening and shifting of the ^1H signals of the thiolate moiety (See Supporting Information Section 3.5), while heating to 60°C also results in sharper signals without a major shift from their position at RT. In addition, the ^{29}Si -INEPT NMR spectrum recorded at -80°C shows a sharp signal at -99.2 ppm that becomes broad at RT and becomes slightly sharper at 60°C at -105.1 ppm, consistent with a temperature-dependent equilibrium between two 5-coordinate species. These observations can be explained by an equilibrium with an ionic form in which the thiophenolate ligand is replaced by a THF molecule (see below). In support of this interpretation, DFT calculation predict a Gibbs free energy of only 5.7 kcal/mol for this ionization process (see Supporting Information Section 5.4).

Compound **4** exhibits a different fluxional process in solution. The ^1H NMR spectrum of **4** in THF-d_8 at room temperature displays two signals at 4.35 and 7.48 ppm that are not bonded to any carbon atom and correspond to the N–H and Si–H moieties, respectively, as well as a series of broad signals belonging to the tmim fragment and the toluidinate moiety. In contrast, a ^1H NMR spectrum of **4** in THF-d_8 at -80°C displays a set of sharp signals consistent

with the crystal structure. An additional set of weaker signals including a bridgehead C–H signal at 5.90 ppm and an indole- CH_3 signal at 2.09 ppm suggest the presence of a minor species in equilibrium. Accordingly, the ^{29}Si NMR spectrum at -80°C also showed two signals at -122.8 ppm ($^1J(^{29}\text{Si}-^1\text{H})=278$ Hz) and at -127.8 ppm ($^1J(^{29}\text{Si}-^1\text{H})=286$ Hz). When warming the sample up to 60°C , the ^1H NMR signals of the tmim fragment and the Si–H (7.45 ppm) become sharp, but the signal of the toluidinate moiety remain significantly broadened, suggesting a larger difference in chemical shift between the two forms. These observations are consistent with the presence of a cisoid conformer in equilibrium with the transoid conformer observed in the solid state (Figure 3), rotation around the Si–NH bond being hindered at low temperature. Because the toluidinate ring is intercalated between indolide rings of the tmim ligand in the cisoid conformer, magnetic shielding by neighboring aromatic ring currents would impact the ^1H signals of the toluidinate more than other signals in the molecule. DFT calculations predict the cisoid conformer to be even slightly lower in energy (-6.4 kcal/mol) than the transoid and afford computed NMR parameters that are in reasonable agreement with experiment (Figure 3).

The low solubility of reactants and products precluded a detailed kinetic study of oxidative addition of X–H bonds to silanide **1** forming compounds **2–4**. Qualitatively, the formation of compounds **2** and **3** is relatively fast (1–2 h) at room temperature, while the formation of compound **4** requires 48 h. This observation suggests that the reaction is faster for more acidic substrates, in line with an ionic mechanism. Replacing the counterion (K[18-crown-6]) in **1** with the thoroughly encapsulated (K[2,2,2-cryptand]) did not strongly inhibit N–H addition to **1**, suggesting no critical role of the potassium counterion in the reaction.

An ionic mechanism is additionally supported by DFT calculations (Scheme 2). In short, compound **1** initially forms H-bonded adducts with the X–H bonds (**7–9**), from which the Si atom is protonated to form ion pairs (**10–12**) that then recombine to form the more stable pentacoordinate products (**2–4**). No transition state could be located for hypothetical concerted oxidative addition processes. However, both protonation and recombination are calculated to be devoid of an electronic barrier, indicating that the energy of

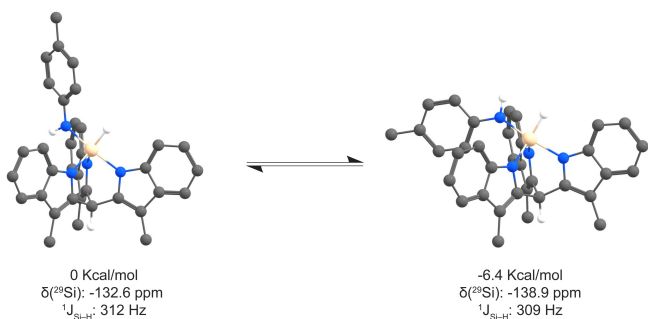
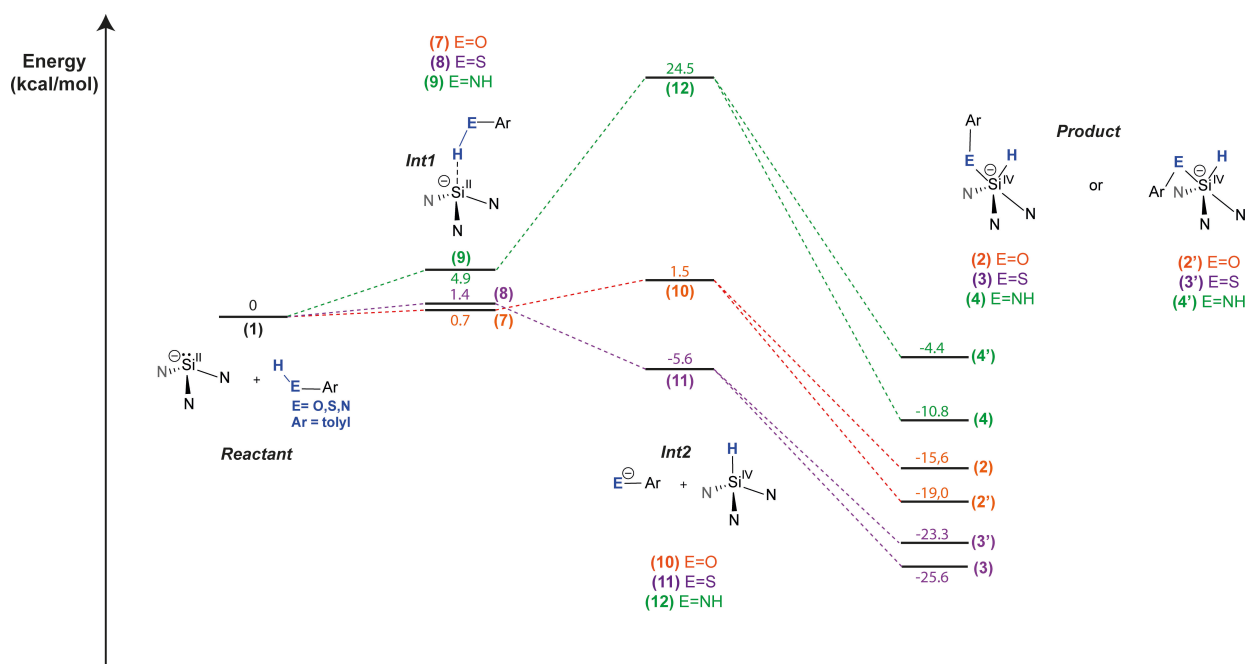


Figure 3. DFT optimized structures for the transoid (left) and cisoid (right) conformers of compound **4** with calculated relative energies and NMR parameters.

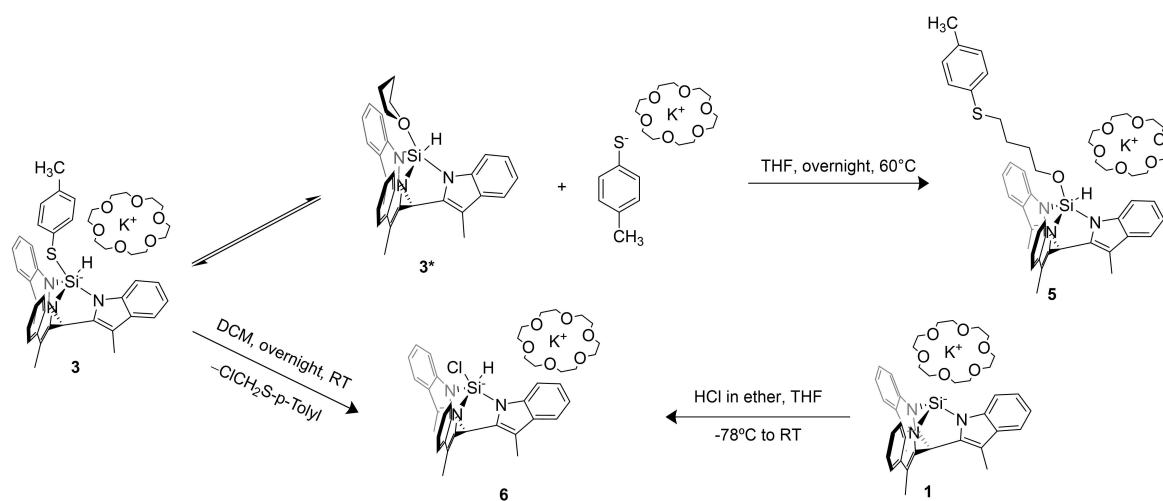


Scheme 2. Computed ionic mechanism for the oxidative addition (B3LYP-GD3BJ/6-311 + G(d,p)//6-31G(d,p)).

the ion pair (10–12) is a good approximation of the overall barrier of the reaction (See Supporting Information section 5.2 for details). In agreement with our observations, the addition of O–H and S–H bonds is predicted to be facile, but the reaction of *p*-toluidine to form compound **4** is energetically more challenging (24.5 kcal/mol). The computed mechanism contrasts with that of O–H addition to silylenes: initial formation of the corresponding Lewis acid–base complex (Si←O–H) followed by H-transfer from the oxygen to the silicon atom. It is also distinct from the concerted oxidative addition of C–F bonds to perfluorinated silanides computed by Hoge et al. Instead, it resembles more that reported for singlet carbenes, which react with

alcohols by initial protonation followed by nucleophilic capture of the resulting carbenium ion.^[33,38]

The thiolate adduct [K(18-crown-6)] [(tmim)SiH-(SC₆H₄CH₃)] (compound **3**) showed peculiar reactivity both in THF and DCM (Scheme 3). In THF, a solvent molecule inserts into the Si–S bond to form compound **5** by ring opening. This process is slow at RT but can be driven to completion by heating a sample to 60 °C overnight. The proposed structure was confirmed using ¹H, ²⁹Si, and 2D NMR data. The ²⁹Si NMR shows coupling with the proton directly bonded to the Si atom (¹J(²⁹Si–¹H) = 302 Hz) but also with the protons of the CH₂ group directly bonded to the oxygen atom (²J(²⁹Si–¹H) = 3 Hz). This result was also



Scheme 3. Reactivity of compound **3**.

confirmed by ^1H - ^{29}Si HMBC (Heteronuclear Multiple Bond Correlation) measurement. Moreover, ^1H - ^{13}C HSQC (Heteronuclear Single Quantum Coherence) and HMBC spectra of **5** are consistent with the proposed structure (see Supporting Information section 3.6). In DCM, compound **3** converts quantitatively to chlorosilicate **6**, in which the thiolate ligand has been substituted by a chloride, one equivalent of chloromethyl-p-tolyl sulfide being formed as by-product (see Supporting Information Section 3.3). The structure of **6** was confirmed by X-ray crystallography (see Figure 2 and Supporting Information Section 3.3). The same compound could be independently synthesized by adding a solution of HCl in ether to a solution of silanide **1** in THF at -78°C . Both reactions can be explained by transient dissociation of the thiophenolate ligand to form the strained, Lewis acidic silane (tmim)SiH that then activates a solvent molecule for nucleophilic attack by the thiophenolate anion. In the case of THF, the solvent adduct **3*** can be observed in equilibrium with compound **3** by variable-temperature NMR (see above).

In summary, we report facile oxidative addition of polar element-hydrogen bonds ($\text{X}-\text{H}$, $\text{X}=\text{O}$, N , S) to a cage silanide, which highlights the potential of silanides as biphilic main-group centers. The resulting hydrosilicates present highly fluxional trigonal bipyramidal structures. The mechanism of the polar $\text{X}-\text{H}$ bond activation was investigated using DFT calculations, which support an ionic mechanism. Moreover, the thiophenol adduct $[\text{K}(18\text{-crown-6})][(\text{tmim})\text{SiH}(\text{SC}_6\text{H}_4\text{CH}_3)]$ reacted with both THF and DCM via transient dissociation of the thiophenolate ligand to reveal a Lewis acidic, neutral silane. These results show that an anionic Si center incorporated in bicyclic cage structure can undergo facile oxidative activation processes connecting the Si^{II} and Si^{IV} oxidation states. The accessibility of such processes is a prerequisite for the future development of catalytic reactions based on the $\text{Si}^{\text{II}}/\text{Si}^{\text{IV}}$ redox couple, which is currently under investigation in our laboratories.

Acknowledgements

This project has received funding from the NoNoMeCat Marie Skłodowska-Curie training network funded by the European Union under the Horizon2020 Program (675020-MSCA-ITN-2015-ETN). The X-ray diffractometer has been financed by the Netherlands Organization for Scientific Research (NWO). This work made use of the Dutch national e-infrastructure with the support of the SURF Cooperative using grants no. EINF-1254 and EINF-3520. The authors thank Prof. R. J. M. Klein Gebbink, Dr. Ing. D. L. J. Broere, and Dr. A. Thevenon for insightful comments. The authors thank C. Zagone for assistance with the design of the TOC graphic.

Conflict of Interest

The authors declare no conflict of interest.

Data Availability Statement

The data that support the findings of this study are available from the corresponding author upon reasonable request.

Keywords: Silanide · Oxidative addition · Small molecule activation · Main-group compounds

- [1] a) C. Weetman, S. Inoue, *ChemCatChem* **2018**, *10*, 4213–4228; b) C. Shan, S. Yao, M. Driess, *Chem. Soc. Rev.* **2020**, *49*, 6733–6754.
- [2] a) F. Ebner, L. Greb, *J. Am. Chem. Soc.* **2018**, *140*, 17409–17412; b) K. M. Marczenko, J. A. Zurakowski, M. B. Kindervater, S. Jee, T. Hynes, N. Roberts, S. Park, U. Werner-Zwanziger, M. Lumsden, D. N. Langelaan, S. S. Chitnis, *Chem. Eur. J.* **2019**, *25*, 16414–16424; c) J. M. Lipshultz, G. Li, A. T. Radosevich, *J. Am. Chem. Soc.* **2021**, *143*, 1699–1721.
- [3] D. W. Stephan, *Acc. Chem. Res.* **2015**, *48*, 306–316.
- [4] A. L. Kenward, W. E. Piers, *Angew. Chem. Int. Ed.* **2008**, *47*, 38–41.
- [5] C. Ganesamoorthy, J. Schoening, C. Wölper, L. Song, P. R. Schreiner, S. Schulz, *Nat. Chem.* **2020**, *12*, 608–614.
- [6] M. J. Krahfuss, U. Radius, *J. Chem. Soc. Dalton Trans.* **2021**, *50*, 6752–6765.
- [7] Y. Xiong, S. Yao, M. Driess, *Chem. Eur. J.* **2009**, *15*, 5545–5551.
- [8] A. Meltzer, S. Inoue, C. Präsang, M. Driess, *J. Am. Chem. Soc.* **2010**, *132*, 3038–3046.
- [9] M. K. Bisai, V. S. V. S. N. Swamy, K. V. Raj, K. Vanka, S. S. Sen, *Inorg. Chem.* **2021**, *60*, 1654–1663.
- [10] Y. Wang, J. Ma, *J. Organomet. Chem.* **2009**, *694*, 2567–2575.
- [11] S. Yadav, S. Saha, S. S. Sen, *ChemCatChem* **2016**, *8*, 486–501.
- [12] F. Roschke, T. Ruffer, H. Lang, M. Mehring, *Z. Anorg. Allg. Chem.* **2018**, *644*, 1361–1366.
- [13] G. C. Nandi, *Eur. J. Org. Chem.* **2021**, *2021*, 587–606.
- [14] Y. Li, B. Ma, C. Cui, *J. Chem. Soc. Dalton Trans.* **2015**, *44*, 14085–14091.
- [15] T. Chu, G. I. Nikonov, *Chem. Rev.* **2018**, *118*, 3608–3680.
- [16] T. Sanji, H. Fujiyama, K. Yoshida, H. Sakurai, *J. Am. Chem. Soc.* **2003**, *125*, 3216–3217.
- [17] S. Ishida, T. Iwamoto, M. Kira, *Organometallics* **2010**, *29*, 5526–5534.
- [18] S. Fujimori, S. Inoue, *Eur. J. Inorg. Chem.* **2020**, *2020*, 3131–3142.
- [19] V. S. V. S. N. Swamy, K. V. Raj, K. Vanka, S. S. Sen, H. W. Roesky, *Chem. Commun.* **2019**, *55*, 3536–3539.
- [20] S. Yao, C. Van Wüllen, X. Y. Sun, M. Driess, *Angew. Chem. Int. Ed.* **2008**, *47*, 3250–3253.
- [21] S. Yao, M. Brym, C. Van Wüllen, M. Driess, *Angew. Chem. Int. Ed.* **2007**, *46*, 4159–4162.
- [22] M. Driess, S. Yao, M. Brym, C. Van Wüllen, D. Lentz, *J. Am. Chem. Soc.* **2006**, *128*, 9628–9629.
- [23] A. C. Tomasik, A. Mitra, R. West, *Organometallics* **2009**, *28*, 378–381.
- [24] N. J. Hill, R. West, *J. Organomet. Chem.* **2004**, *689*, 4165–4183.
- [25] P. D. Prince, M. J. Bearpark, G. S. McGrady, J. W. Steed, *J. Chem. Soc. Dalton Trans.* **2007**, 271–282.
- [26] Z. Benedek, T. Szilvási, *RSC Adv.* **2015**, *5*, 5077–5086.
- [27] L. Witteman, T. Evers, M. Lutz, M. E. Moret, *Chem. Eur. J.* **2018**, *24*, 12236–12240.
- [28] V. D. Thalangamaarachchige, D. K. Unruh, D. B. Cordes, C. Krempner, *Inorg. Chem.* **2015**, *54*(9), 4189–4191.
- [29] M. W. Stanford, A. Bismuto, M. J. Cowley, *Chem. Eur. J.* **2020**, *26*, 9855–9858.

- [30] T. Thorwart, D. Roth, L. Greb, *Chem. Eur. J.* **2021**, *27*, 10422–10427.
- [31] A. L. Liberman-Martin, R. G. Bergman, T. D. Tilley, *J. Am. Chem. Soc.* **2015**, *137*, 5328–5331.
- [32] J. C. Lindon, G. E. Tranter, D. Koppenaal, in *Encyclopedia of Spectroscopy and Spectrometry*, Elsevier Science, **2016**.
- [33] N. Tiessen, M. Keßler, B. Neumann, H. Stammler, B. Hoge, *Angew. Chem. Int. Ed.* **2022**, *61*, e202116468.
- [34] N. Tiessen, M. Keßler, B. Neumann, H. G. Stammler, B. Hoge, *Angew. Chem. Int. Ed.* **2021**, *60*, 12124–12131.
- [35] S. Tretiakov, L. Witteman, M. Lutz, M. E. Moret, *Angew. Chem. Int. Ed.* **2021**, *60*, 9618–9626.
- [36] N. Rot, T. Nijbacker, R. Kroon, F. J. J. De Kanter, F. Bickelhaupt, M. Lutz, A. L. Spek, *Organometallics* **2000**, *19*, 1319–1324.
- [37] E. P. A. Couzijn, J. C. Slootweg, A. W. Ehlers, K. Lammertsma, *J. Am. Chem. Soc.* **2010**, *132*, 18127–18140.
- [38] W. J. Leigh, S. S. Kostina, A. Bhattacharya, A. G. Moiseev, *Organometallics* **2010**, *29*, 662–670.
- [39] Deposition Number(s) 2293010 (for **2a**), 2293011 (for **3**), 2293012 (for **4**), 2293013 (for **6**), 2293014 (for [(18-crown-6)K]⁺[(PhO)(tmimH₃)]⁻) contain(s) the supplementary crystallographic data for this paper. These data are provided free of charge by the joint Cambridge Crystallographic Data Centre and Fachinformationszentrum Karlsruhe Access Structures service .
- Manuscript received: December 22, 2023
Accepted manuscript online: January 16, 2024
Version of record online: February 5, 2024